Oncology Research, Vol. 28, pp. 779–790
Printed in the USA.

0965-0407/21 $90.00 + .00
DOI: https://doi.org/10.3727/096504021X16161478258040
E-ISSN 1555-3906
www.cognizantcommunication.com

TBK1 Inhibitor Exerts Antiproliferative Effect on Glioblastoma Multiforme Cells

Sarah A. Scuderi,* Marika Lanza,* Giovanna Casili,* Francesca Esposito,† Cristina Colarossi,‡ Dario Giuffrida,‡ Paterniti Irene,* Salvatore Cuzzocrea,* Emanuela Esposito,* and Michela Campolo*

*Department of Chemical, Biological, Pharmaceutical and Environmental Sciences, University of Messina, Messina, Italy
†IOM Ricerca Srl, Viagrande, Italy
‡Istituto Oncologico del Mediterraneo Spa, Viagrande, Italy

Glioma are common malignant brain tumors, among which glioblastoma multiforme (GBM) has the worst prognosis. Different studies of GBM revealed that targeting nuclear factor B (NF- B) induced an attenuation tumor proliferation and prolonged cell survival. TBK1 {TANK [TRAF (TNF (tumor-necrosis-factor) receptor-associated factor)-associated NF- B activator]-binding kinase 1} is a serine/threonine protein kinase, and it is a member of the I B kinase (IKK) family involved in NF- B pathway activation. The aim of this study was to investigate the potential effect of BX795, an inhibitor of TBK1, in an in vitro and ex vivo model of GBM. GBM cell lines (U87 and U138) and primary GBM cells were treated with different concentrations of BX795 at different time points (24, 48, and 72h) to evaluate cell viability, autophagy, inflammation, and apoptosis. Our results demonstrated that BX795 10 μM was able to reduce cell viability, showing antiproliferative effect in U87, U138, and primary GBM cells. Moreover, treatment with BX795 10 μM increased the proapoptotic proteins Bax, p53, caspase 3, and caspase 9, whereas the antiapoptotic Bcl-2 expression was reduced. Additionally, our results showed a marked decrease in autophagy following BX795 treatment, reducing Atg 7, Atg 5/12, and AKT expression. The anti-inflammatory effect of BX795 was demonstrated by a significantly reduction in NIK, IKK , and TNF- expression, accompanied by a downregulation of angiogenesis. Furthermore, in primary GBM cell, BX795 10 μM was able to reduce TBK1 pathway activation and SOX3 expression. In conclusion, these findings showed that TBK1 is involved in GBM proliferation, demonstrating that the inhibitor BX795, thanks to its abilities, could improve therapeutic strategies for GBM treatment.

Key words: Glioblastoma multiforme (GBM); TBK1 (TANK-binding kinase); Nuclear factor kappa-light-chain-enhancer of activated B cells (NF-κB); IκB kinase subunit epsilon (IKKε)

INTRODUCTION

Gliomas are common malignant brain tumors, among which glioblastoma multiforme (GBM) has the worst prognosis[1]. GBM is the most common and aggressive malignant tumor of the central nervous system, characterized by a high degree of proliferation, angiogenesis, necrosis, and invasiveness[2]. GBM is associated with chromosomal and genetic mutations that determine the uncontrolled growth of brain cells and tumor cell chemoresistance[3,4]. The current standard treatment for GBM consists of surgical resection, followed by radiotherapy with concomitant and adjuvant temozolomide (TMZ) chemotherapy[5]. However, the survival rate for GBM patients remains low[6]; therefore, the identification of new therapeutic targets represents an important goal for oncology research. TBK1 (TANK-binding kinase) is a serine/threonine protein kinase encoded by the tbk1 gene; it is a member of the IKB kinase (IKK) family[7]. The binding between IKK (I B kinase), a key component of nuclear factor B (NF- B) signaling, and TBK1 promotes NF- B and interferon regulatory factor (IRF) signaling pathway activation. This link consequently promotes autophagy and inflammatory process through the activation of important factors involved in cancer development, including protein kinase B (Akt) and factor 2 (TRAF2) associated with the necrosis factor receptor tumor (TNF-R)[7], and inhibiting tumor suppressors such as cylindramatosis tumor suppressor (CYLD) and Forkhead box O3a (FoxO3a)[8]. TBK1 showed greater expression in solid tumors; in

Address correspondence to Prof. Emanuela Esposito, Department of Chemical, Biological, Pharmaceutical and Environmental Sciences, University of Messina, Viale Ferdinando Stagno D' Alcontres, No. 31, 98166 Messina, Italy. Tel: (39) 090-6765208; E-mail: eesposito@unime.it

this context, TBK1 promotes cancer cell survival and tumor growth through apoptosis pathway alteration, and it induces proinflammatory cytokine production through NF- B pathway activation[9]. Recent studies have revealed the possible use of BX795, a specific TBK1 inhibitor for the treatment of many cancer types, as primary pancreatic ductal adenocarcinoma and melanoma[10,11]. BX795 was originally identified as a 3-phosphoinositide-dependent protein kinase (PDK1) inhibitor, but it has been shown to inhibit mostly TBK1 and IKK [12], showing anti-inflammatory effect. Furthermore, BX795 is able to suppress the activity of the regulatory factor for interferon 3 (IFN3) and also the production of interferon- (IFN-) in macrophages[12]. Therefore, this study aims to evaluate the effects of BX795 in the processes of inflammation, autophagy, and apoptosis in in vitro and ex vivo studies of GBM.

MATERIALS AND METHODS

In Vitro Studies

Cell Lines. The human GBM cell lines U-138MG (U-138 MG ATCC® HTB-16™ *Homo sapiens* brain glioblastoma) and U-87 MG (U-87 MG ATCC® HTB-14™ *Homo sapiens* brain Likely glioblastomas) were obtained from the ATCC (American Type Culture Collection, Rockville, MD, USA). Cell lines U-138 and U-87 were derived from human malignant gliomas and are commonly used as experimental models of glioblastoma[13,14]. U-138 differs from U-87 in morphology, invasion, and proliferation rate[13]. U-138 and U-87 exhibit different protein expression profiles, mainly characterized by a very low expression of glial fibrillary acidic protein (GFAP), generally expressed in glial cells and almost completely absent in U-87 cells[15,16]. GBM cells lines were cultured in a 75-cm^2 flask with, respectively, ATCC-formulated Eagle's Minimum Essential Medium (Catalog No. 30-2003; ATCC) for U-138 MG and Dulbecco's modified Eagle's medium (DMEM; Catalog No. D5030; Sigma-Aldrich, St. Louis, MO, USA) for U-87 MG, both supplemented with antibiotics (penicillin, 1000 U; streptomycin, 0.1 mg/L; Catalog No. P4333; Sigma-Aldrich), L-glutamine (GlutaMAX™, Catalog No. 35050061; ThermoFisher Scientific, Waltham, MA, USA), and 10% (v/v) fetal bovine serum (FBS; Catalog No. 12103C; Sigma-Aldrich) in a humidified atmosphere containing 5% CO_2 at 37° C.

Cell Treatment. U-87 MG and U-138 MG cells were cultured in six-well culture plates at a density of 2.5 × 10^5 cells/well. Sixteen hours after seeding, a set of plates were treated with BX795 (Catalog No. 204001; Sigma-Aldrich) at increasing concentrations of 0.1, 0.5, 1, and 10 μM dissolved in dimethyl sulfoxide (DMSO) (20 mg/ml; sc-358801; Santa Cruz Biotechnology, Dallas, TX, USA) for a time from 24 to 72 h. The IC_{50} values were calculated by fitting the progress curves to the three parameters using GraphPad Prism software version 7.0 (GraphPad Software, La Jolla, CA, USA).

Experimental Groups. (1) Control (Ctr): human GBM cell lines U-87 MG and U-138 MG; (2) BX795 0.1 μM group: GBM cell lines U-87 MG treated with 0.1 μM BX795; (3) BX795 0.5 μM group: GBM cell lines U-87 MG treated with 0.5 μM BX795; (4) BX795 1 μM group: GBM cell lines U-87 MG treated with 1 μM BX795; and (5) BX795 10 μM group: GBM cell lines U-87 MG treated with 10 μM BX795.

MTT Assay. Cell viability was measured using a mitochondria-dependent dye for live cells (tetrazolium dye; MTT) (M5655; Sigma-Aldrich) as previously described by Esposito et al.[17]. U-87 MG and U-138 MG cells were pretreated with increasing concentrations of BX795 (0.1, 0.5, 1, and 10 μM) to determine high concentrations with high toxicity on cell viability. After 24 h, cells were incubated at 37°C with MTT (0.2 mg/ml) for 1 h. The medium was removed by aspiration, and the cells were lysed with DMSO (100 μl). The extent of reduction of MTT to formazan was quantified by measurement of optical density at 550 nm (OD550) with a microplate reader[18].

RNA Isolation, cDNA Synthesis, and Real-Time Quantitative Polymerase Chain Reaction (PCR) Amplification. Total RNA was isolated from U-87 cells for RT-qPCR analysis using a TRIzol Reagent Kit (Life Technologies, Monza, Italy) as previously described[19]. The first strand of cDNA was synthesized from 2.0 μg of total RNA using a high-capacity cDNA Archive kit (Applied Biosystems, Carlsbad, CA, USA). RT-qPCR was performed to evaluate the gene expression of Bcl-2, BAX, p53, caspase 3, caspase 9, autophagy-related (Atg) 5/12, Atg 7, AKT, and p62/SQSTM1 using Power Up Sybr Master Mix (Applied Biosystems) and a QuantStudio 6 Flex Real-Time PCR System (Applied Biosystems). The amplified PCR products were quantified by measuring the calculated cycle thresholds (CT) of target genes and -actin mRNA. -Actin mRNA was used as an endogenous control to allow for the relative quantification. After normalization, the mean value of the normal control target levels was chosen as the calibrator, and the results were expressed as a fold change relative to normal controls. The oligonucleotide sequences of the used primers are reported in Table 1.

Western Blot Analysis. Western blot analysis was performed as previously described[20]. U-87 cells were washed twice with ice-cold phosphate-buffered saline (PBS), harvested, and resuspended in Tris-HCl 20 mM pH 7.5, NaF 10 mM, 150 μl of NaCl, 1% Nonidet P-40, and protease inhibitor cocktail (Catalog No. 11836153001; Roche, Switzerland). After 40 min, cell lysates were centrifuged

Table 1. Primer Sequences Used for RT-qPCR

Gene	Forward Primer 5 −3	Reverse Primer 5 −3
Bcl-2	GAGGATTGTGGCCTTCTTTGAG	AGCCTCCGTTATCCTGGATC
Bax	GGACGAACTGGACAGTAACATG	GCAAAGTAGAAAAGGGCGACA
P53	AGAGTCTATAGGCCCACCCC	GCTCGACGCTAGGATCTGAC
Caspase 3	CTGAGGCATGGTGAAGAAGGA	GTCCAGTTCTGTACCACGGCA
Caspase 9	TGCGAACTAACAGGCAAGCA	GTCTGAGAACCTCTGGTTTGC
Atg 5/12	ATGACTAGCC-GGGACACC	CCAGTTTAC-CATCACTGCC
Atg 7	TTCTGTTCCCTCAGCGTGTC	GCCAGTCTCTTTGGGTCCAT
AKT	TCT ATG GCG CTG AGA TTGTG	CTT AAT GTG CCC GTC CTTGT
P62/SQSTM1	GCAUUGAAGUUGAUAUCGAUTT	ACAGAUGGAGUCGGAUAAC
-Actin	GACTTCGAGCAAGAGATGG	AGCACTGTGTTGGCGTACAG

at 12,000 rpm for 15 min at 4°C. Protein concentration was estimated by the Bio-Rad protein assay (Bio-Rad Laboratories, Hercules, CA, USA) using bovine serum albumin as standard. Samples were then heated at 95°C for 5 min, and equal amounts of protein were separated on a 10%–15% sodium dodecyl sulfate-polyacrylamide gel electrophoresis (SDS-PAGE) gel and transferred to a polyvinylidene difluoride (PVDF) membrane (Immobilon-P, Catalog No. 88018; ThermoFisher Scientific). The following primary antibodies were used: anti-IRF3 (1:500; ab68481; Abcam, Cambridge, MA, USA), anti-VEGF (vascular endothelial growth factor) (1:500; sc-7269; Santa Cruz Biotechnology), anti-NIK (NF- B-inducing kinase) (1:500; sc-8417; Santa Cruz Biotechnology), anti-I B kinase (IKK) (1:500; sc-7606; Santa Cruz Biotechnology), anti-Bax (1:500; sc-7480; Santa Cruz Biotechnology), anti-Bcl2 (1:500; sc-7382; Santa Cruz Biotechnology), anti-p53 (1:500; sc-126; Santa Cruz Biotechnology), anti-caspase 3 (1:500; sc-7272; Santa Cruz Biotechnology), and anti-caspase 9 (1:500; sc-73548; Santa Cruz Biotechnology). Antibody dilutions were made in PBS/5% w/v nonfat dried milk/0.1% Tween-20 (PMT), and membranes were incubated overnight at 4°C. Membranes were then incubated with secondary antibody (1:2000; Jackson ImmunoResearch, West Grove, PA, USA) for 1 h at room temperature. To ascertain that blots were loaded with equal amounts of protein lysate, they were also incubated with -actin antibody (cytosolic fraction 1:500; sc-47778; Santa Cruz Biotechnology) or lamin A/C (nuclear fraction 1:500; sc-376248; Santa Cruz Biotechnology). Signals were detected as previously described[21].

Enzyme-Linked Immunosorbent Assay (ELISA) Assay for Tumor Necrosis Factor-α (TNF-α) and IFN-β. The levels of TNF- and IFN- in U-87 cells were performed by ELISA kit as previously described[22] (mouse TNF- ELISA kit; Cat. No. ab100654; Abcam; mouse IFN- ELISA kit; Cat. No. ab252363; Abcam). In brief, cells from each group were seeded into 96-well plates at a density of 1×10^4 cells/well and were cultured for 24 h. Cultures in serum-free medium were incubated in 5% CO_2 at 37°C for 24 h. The culture medium was then collected and assayed according to the manufacturer's instructions. Absorbance detection was performed at 450 nm using a microplate reader (model 550; Bio-Rad Laboratories Inc.).

Statistical Analysis. All values are expressed as mean ± standard error of the mean (SEM) of *n* observations. Each analysis was performed three times with three samples replicates for each one. The results were analyzed by one-way analysis of variance (ANOVA) followed by a Bonferroni post hoc test for multiple comparisons. A value of $p < 0.05$ was considered significant.

Ex Vivo Studies

Primary GBM Cell Culture. Primary tumor GBM cells from patients were obtained according to protocol approved by the Regional Ethical Board at the University of Messina. All subjects gave their informed consent for inclusion before they participated in the study. The study was conducted in accordance with the Declaration of Helsinki, and the protocol was approved by the Ethics Committee of AOU "G. Martino," Hospital of Messina (No. 47/19 of 05/02/2019). Tumor samples were processed aseptically, and primary cell cultures were initiated using DMEM (Catalog No. D5030; Sigma-Aldrich) with 15% heat-inactivated fetal calf serum (FCS) (Catalog No. 12103C; Sigma-Aldrich), 2 mM GlutaMAX-I (Catalog No. 35050061; ThermoFisher Scientific), 1% insulin-transferrin-selenium-X supplement (Catalog No. 41400045; ThermoFisher Scientific), and 1% penicillin-streptomycin mixture (Catalog No. 15640055; Invitrogen, Carlsbad, CA, USA). Cells were used within 7 days of plating or established as primary cell lines.

Experimental Groups. (1) Control (Ctr): healthy brain tissues were processed and used as negative control; (2) primary GBM cell: tumor cells obtained from patients were processed and used as positive control; and (3)

BX795 10 μM cell: glioblastoma cells from patients were treated with BX795 at concentration of 10 μM.

MTT Assay. Primary GBM cell culture obtained from patients was treated with BX795 at a concentration of 10 μM. After 24 h, primary GBM cells were incubated at 37°C with MTT (0.2 mg/ml; M5655; Sigma-Aldrich) for 1 h. The medium was removed by aspiration, and the cells were lysed with 100 μl of DMSO (sc-358801; Santa Cruz Biotechnology). The extent of reduction of MTT to formazan was quantified by measurement of optical density at 550 nm (OD550) with a microplate reader[18].

Western Blot Analysis. Protein extraction and Western blot analysis in primary GBM cell culture were performed as previously described[20]. The filters were probed with specific antibodies: anti-TBK1 (1:500; sc-52957; Santa Cruz Biotechnology), anti-SOX3 (1:500; sc-101155; Santa Cruz Biotechnology), anti-IRF3 (1:500; ab68481; Abcam), and anti-IFN- (1:500; sc-390800; Santa Cruz Biotechnology) in 1 × PBS, 5% w/v nonfat dried milk (sc-2324; Santa Cruz Biotechnology), 0.1% Tween-20 (P9416; Sigma-Aldrich) at 4°C overnight. The day after, the membranes were incubated with a specific peroxidase-conjugated secondary antibody (Pierce, Cramlington, UK) for 1 h at room temperature and were analyzed by KPL enhanced chemiluminescence (ECL) (SeraCare, Pittsburgh, PA, USA). Protein signals were quantified by scanning densitometry using a bio-image analysis system (Bio-Profil, Milan, Italy), and the results were expressed as relative integrated intensity compared to controls. To ascertain that blots were loaded with equal amounts of proteins, they were also incubated in the presence of the antibody against -actin protein (cytosolic fraction 1:500; sc-47778; Santa Cruz Biotechnology). Signals were detected with ECL detection system reagent according to the manufacturer's instructions (ThermoFisher Scientific). The relative expression of the protein bands was quantified by densitometry with Bio-Rad ChemiDoc XRS+ software. Images of blot signals (8 bit/600 dpi resolution) were imported to the analysis software (Image Quant TL, v2003).

Statistical Analysis. All values are expressed as mean ± SEM of *n* observations. Each analysis was performed three times with three samples replicates for each one. The results were analyzed by one-way ANOVA followed by a Bonferroni post hoc test for multiple comparisons. A value of $p < 0.05$ was considered significant.

RESULTS

In Vitro Studies

Effects of BX795 on Cell Viability. BX795 cytotoxicity was evaluated incubating cell lines U-138 and U-87 with growing concentrations of BX795 (0.1, 0.5, 1, and 10 μM). BX795 treatment showed cytotoxic and antiproliferative effects at 24, 48, and 72 h from the beginning of the treatment in U-138 and U-87 in a concentration- and time-dependent manner (Figs. 1A and B and 2A and B). The values of 1 and 10 μM represented the most cytotoxic concentrations of BX795 as shown in Figures 1A and B and 2A and B. The IC_{50} values for U-87 cells are included in the range of 3.5 to 0.32, and for U-138 cells, IC_{50} values range from 4.4 to 1.04.

Effects of BX795 on Apoptosis. Apoptosis-inducing therapies have gained a great interest as promising experimental treatment strategies for GBM[23]. Therefore, we investigated the potential effect of BX795 on apoptosis pathway, especially on Bax, Bcl-2, p53, caspase 3, and caspase 9 expression. U-87 cells were treated with 1 and 10 μM BX795 and analyzed by RT-qPCR. The results showed a significantly increase in the concentration of 10 μM proapoptotic Bax (Fig. 3A) and tumor suppressor p53 mRNA expression (Fig. 3B) and a reduction in Bcl-2 mRNA expression (Fig. 3C). In addition, the results obtained were confirmed by Western blot analysis,

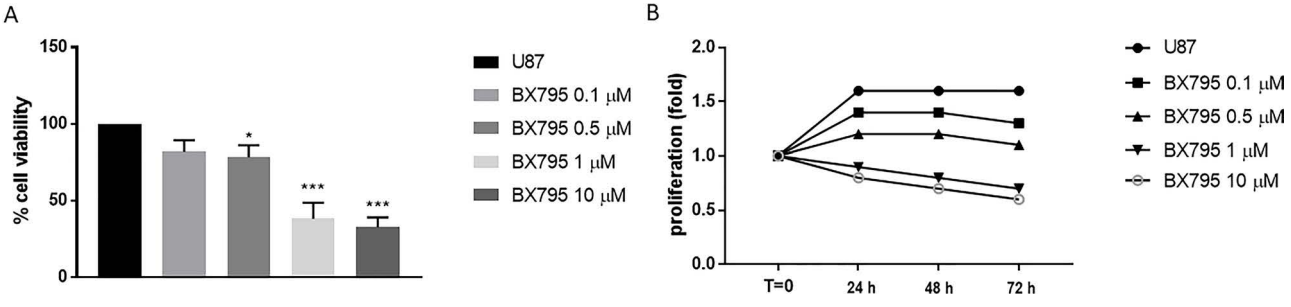

Figure 1. Effect of BX795 on cell viability in U-87 cells. Cell viability was evaluated using MTT assay 24 h after BX795 treatment at the concentrations of 0.1, 0.5, 1 and 10 μM. U-87 cells showed a decrease in proliferation following BX795 treatment in a concentration-dependent manner, mostly at the concentrations of 1 and 10 μM (A). Cell proliferation was evaluated at T0, 24, 48, and 72 h in U-87 cells, demonstrating that BX795 treatment was able to suppress cell proliferation (B). Data are representative of at least three independent experiments. *$p < 0.05$, ***$p < 0.001$ versus the control group.

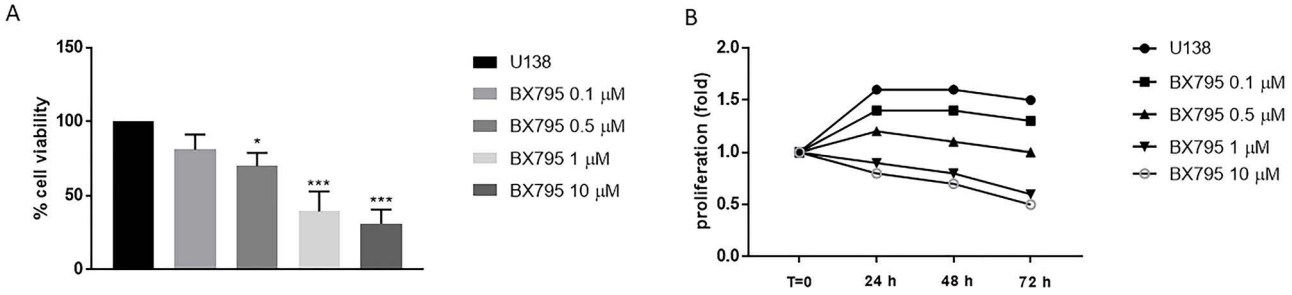

Figure 2. Effect of BX795 on cell viability in U-138 cells. Cell viability was evaluated using MTT assay 24 h after BX795 treatment at the concentrations of 0.1, 0.5, 1 and 10 μM. U-138 cells showed a significant decrease in proliferation following BX795 treatment in a concentration-dependent manner, mostly at the concentrations of 1 and 10 μM (A). Cell proliferation was evaluated at T0, 24, 48, and 72 h in U-138 cells, demonstrating that BX795 treatment was able to suppress cell proliferation (B). Data are representative of at least three independent experiments. *$p < 0.05$, ***$p < 0.001$ versus the control group.

confirming an increase in Bax and p53 expression and a decrease in Bcl-2 expression after BX795 10 μM treatment (Fig. 3D–F, respectively). Moreover, BX795 treatment at the concentration of 10 μM induced a significant increase in caspase 3 and caspase 9 mRNA expression (Fig. 4A and B), highlighting an apoptosis activation. These results were confirmed also by Western blot analysis as shown in Figures 4C and D, respectively.

Effects of BX795 on Autophagy. Loss of the autophagy-related (Atg) genes is frequently associated with cancer induction and development, suggesting tumor suppressor-like role of autophagy in cancer[24,25]. Therefore, we investigated the ability of BX795 treatment in U-87 cells to act on the autophagy pathway by evaluating Atg 5/12, Atg 7, AKT, and p62/SQSTM1 (sequestome 1) expression, an autophagy adaptive protein, by RT-qPCR. The results demonstrated that BX795 treatment at the concentration of 10 μM significantly reduced Atg 5/12, Atg 7, AKT, and p62/SQSTM1 mRNA expression as shown in Figure 5A–D, respectively.

Effects of BX795 on Inflammation. In the context of GBM, various studies have focused on the NF- B pathway activation, which is related to IKK and NIK (also known as MAP3K14) activation, leading to the

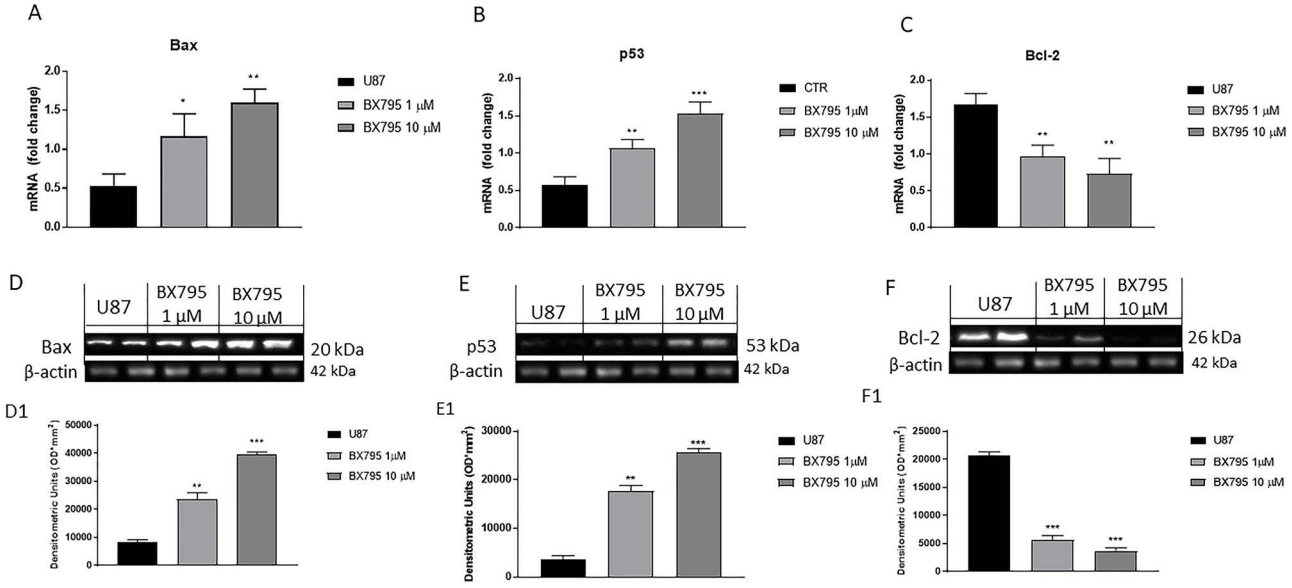

Figure 3. Effect of BX795 on apoptosis pathway. Treatment with BX795 at the concentrations of 1 and 10 μM significantly increased Bax and p53 mRNA expression (A, B) and reduced Bcl-2 mRNA expression (C) in U-87 cells compared to the control group evaluated by real-time quantitative polymerase chain reaction (RT-qPCR). Moreover, Western blot analysis confirmed an increase in Bax (D) and p53 expression (E) and a reduction in Bcl-2 (F). Data are representative of at least three independent experiments. *$p < 0.05$, **$p < 0.01$, ***$p < 0.001$ versus control.

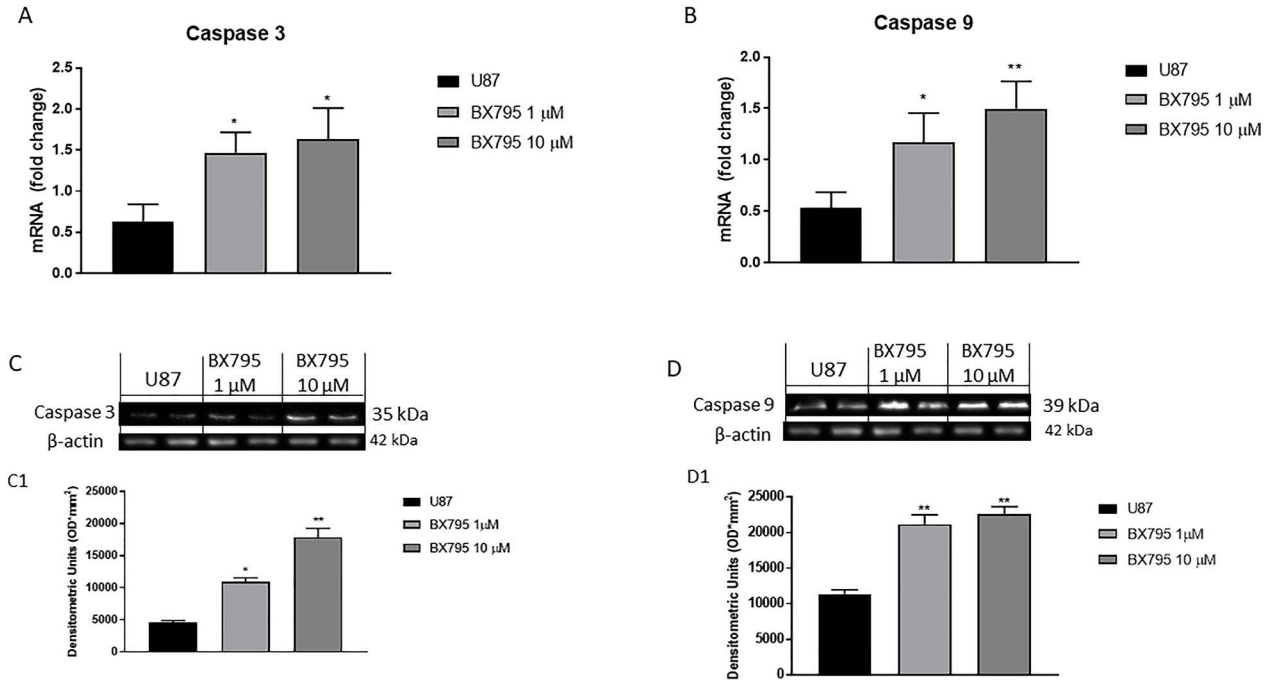

Figure 4. Effect of BX795 on caspase 3 and caspase 9 activation. BX795 treatment was demonstrated at the concentrations of 1 and 10 μM to induce caspase 3 (A) and caspase 9 (B) mRNA expression in U-87 cells. In addition, Western blots analysis confirmed an increase in caspase 3 (C) and caspase 9 expression (D) after BX795 treatment. Data are representative of at least three independent experiments. $*p < 0.05$, $**p < 0.01$ versus control.

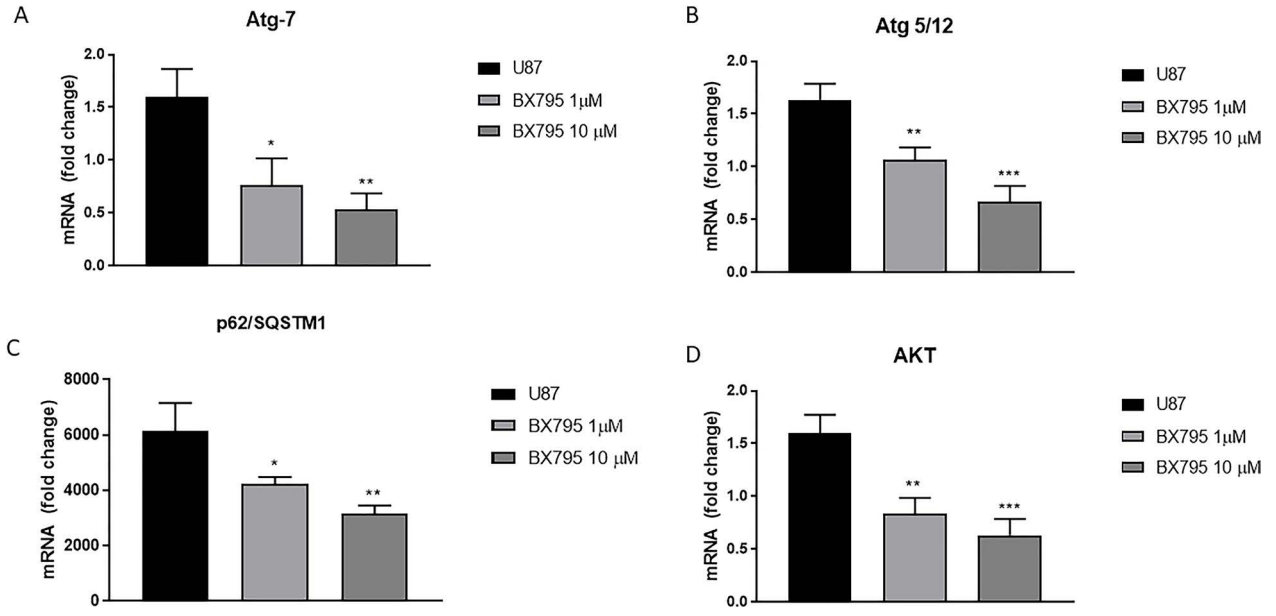

Figure 5. Effect of BX795 on autophagy. The graphs represent Atg 7 (A), Atg 5/12 (B), p62/SQSTM1 (C), and AKT (D) mRNA expressions in U-87 cells. Treatment with BX795 significantly reduced Atg 7, Atg 5/12, p62/SQSTM1, and AKT protein expression in U-87 cells compared to control group. Data are representative of at least three independent experiments $*p < 0.05$, $**p < 0.01$, $***p < 0.001$ versus control.

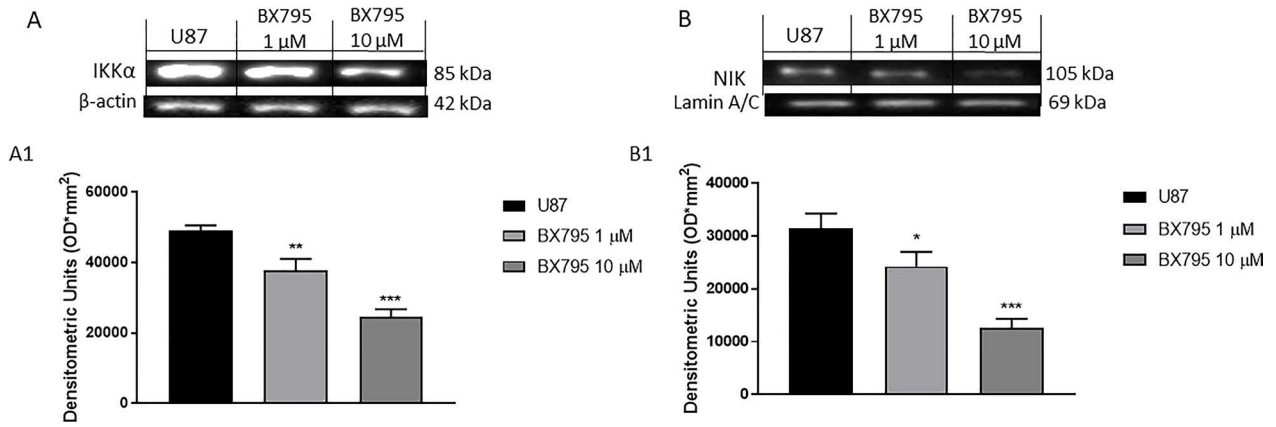

Figure 6. Effect of BX795 on I B kinase (IKK) and NF- B-inducing kinase (NIK) pathway. Blots revealed a significant increase in IKK (A) and NIK (B) in U-87 cells. Meanwhile, their expressions were significantly attenuated in the groups treated with 1 and 10 μM BX795, reducing the inflammation process. Data are representative of at least three independent experiments. *$p < 0.05$, **$p < 0.01$, ***$p < 0.001$ versus control.

release of proinflammatory cytokines such as TNF- and IFN- [26]. Therefore, in this study, we investigated the anti-inflammatory effects of BX795 in U-87 cells. The results demonstrated that BX795 treatment at the concentrations of 1 and 10 μM significantly reduced IKK and NIK expression, as evaluated by Western Blot analysis (Fig. 6A and B, respectively), as well as the reduced TNF- and IFN- levels, as evaluated by ELISA assay (Fig. 7A and B, respectively).

Effects of BX795 on Angiogenesis. GBM tumors are highly vascularized, and glioma growth depends on the formation of new blood vessels. Thus, in this study, we investigated the role of the VEGF[27] and of the transcription factor interferon regulatory factor 3 (IRF3) that are involved in glioma invasiveness, proliferation, and production of proinflammatory and proangiogenic mediators[28]. The obtained results demonstrated the ability of BX795 to reduce the angiogenesis process in U-87 cells by Western blot analysis. The results showed a significant increase in VEGF and IRF3 expression in GBM cell, while BX795 treatment significantly downregulated IRF3 and VEGF expression at concentrations of 1 and 10 μM, as shown in Figure 8A and B.

Ex Vivo Studies

Effects of BX795 on Cell Viability in Primary GBM Cell Culture. BX795 cytotoxicity was evaluated in primary GBM cell culture obtained from patients at the concentration of 10 μM, which represented the most effective concentration. BX795 treatment showed a reduction in

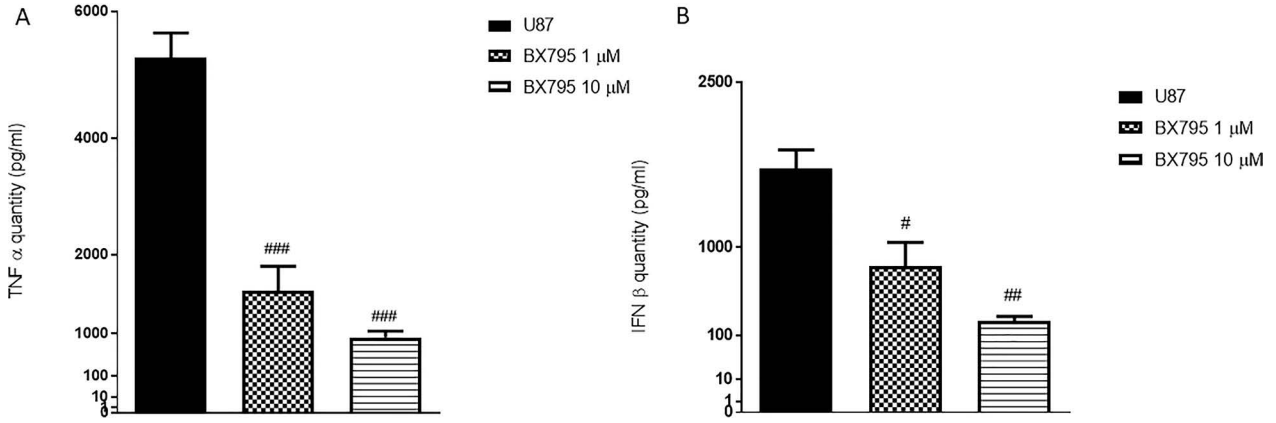

Figure 7. Effects of BX795 on tumor necrosis factor- (TNF-) and interferon- (IFN-) expressions in U-87 cells. An increase in TNF- (A) and IFN- (B) levels was evident in U-87 cells, while the treatment with BX795 at the concentrations of 1 and 10 μM significantly reduced their expression, relieving inflammation. Data are representative of at least three independent experiments. #$p < 0.05$, ##$p < 0.01$, ###$p < 0.001$ versus control.

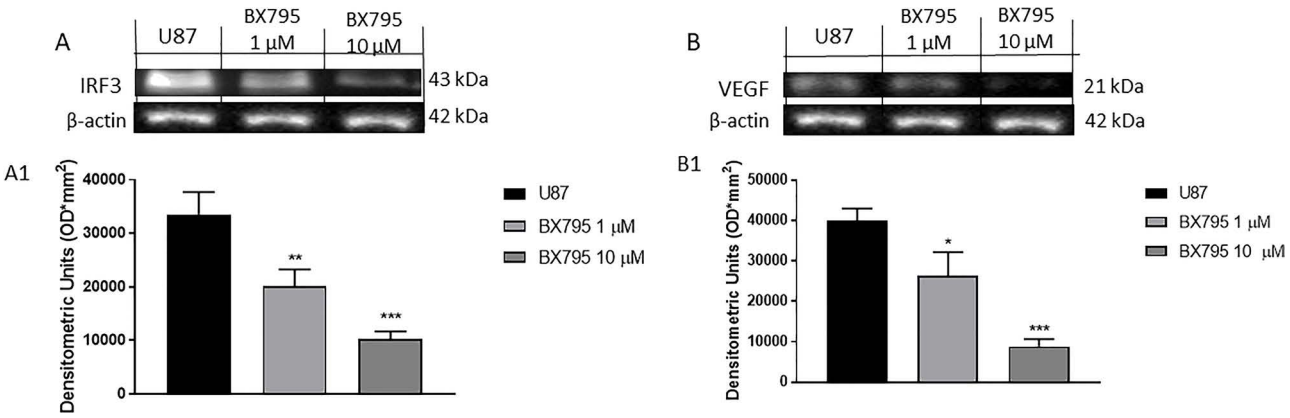

Figure 8. Effect of BX795 on angiogenesis. Blots revealed an increase in IRF3 (A) and vascular endothelial growth factor (VEGF) (B) expression in U-87 cells. Meanwhile, BX795 treatment significantly reduced their expression at the concentrations of 1 and 10 μM in a concentration-dependent manner, demonstrating reduction in angiogenesis process. Data are representative of at least three independent experiments. *$p < 0.05$, **$p < 0.01$, ***$p < 0.001$ versus control.

cell viability in primary GBM cells (Fig. 9A) and antiproliferative effect at the concentration of 10 μM for indicated time intervals (Fig. 9B).

Effects of BX795 on TBK1, IRF3, IFNγ, and SOX3 Expression in Primary GBM Cell Culture. To validate the effective role of the use of TBK1 inhibitor in glioblastoma cell patients, we assessed Western blot analysis for TBK1. As shown in Figure 10A, an increase in TBK1 expression was found in primary cells extracted from patients with GBM compared with control; BX795 at the concentration of 10 μM was able to significantly reduce TBK1 expression.

To confirm the potential effect of BX795 inhibitor on primary GBM cells obtained from patients, we investigated by Western blot analysis IRF3 and IFN- expression, two key proteins phosphorylated by TBK1[29]. The results obtained showed an increase in IRF3 and IFN- expression in primary GBM cells, meanwhile BX795 10 μM treatment significantly reduced their expression as shown in Figure 10B and C.

Numerous studies have shown that some transcription factors such as SOX3 are capable of acting as oncogenes by promoting the acquisition of tumor stem cell-like phenotypes in GBM[30,31]. Many studies demonstrated that SOX3 overexpression induces an increase in cell viability, proliferation, migration, and invasion of GBM cells[31]. Therefore, in this study, we evaluated SOX3 expression in primary GBM cell culture by Western blot analysis. We found that SOX3 expression in the primary GBM cell culture was higher than that in the control; however, BX795 treatment at the concentration of 10 μM significantly reduced SOX3 expression as shown in Figure 10D.

DISCUSSION

GBM is the most common and aggressive malignant tumor of the central nervous system[32]. GBM is characterized by diffuse infiltration of the brain tissue surrounding the bulk of the tumor[3,6]. Although the clinical treatment options are multiple and effective, the survival rate for patients with GBM remains low and additional therapies

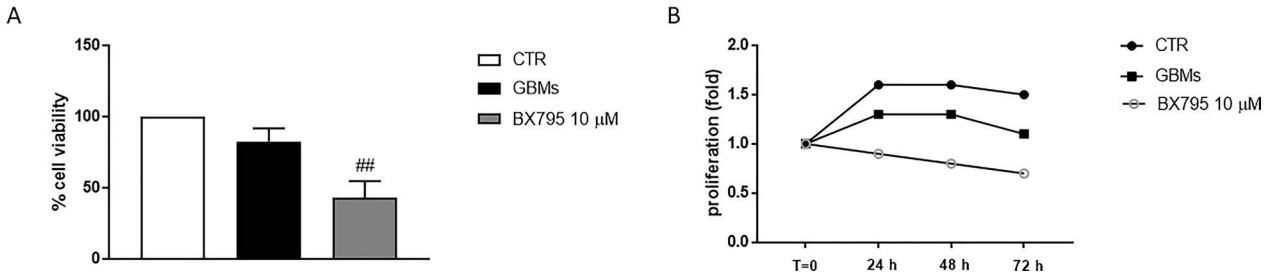

Figure 9. Effect of BX795 on cell viability in primary glioblastoma multiforme (GBM) cell culture. Cell viability was evaluated using MTT assay 24 h after BX795 treatment at the concentration of 10 μM. The result demonstrated that 10 μM BX795 treatment reduced cell viability in primary GBM cells (A). Cell proliferation was evaluated at T0, 24, 48, and 72 h in primary GBM cell. BX795 treatment 10 μM was able to suppress cell proliferation compared to the control group (B). Data are representative of at least three independent experiments. ##$p < 0.01$ versus GBM.

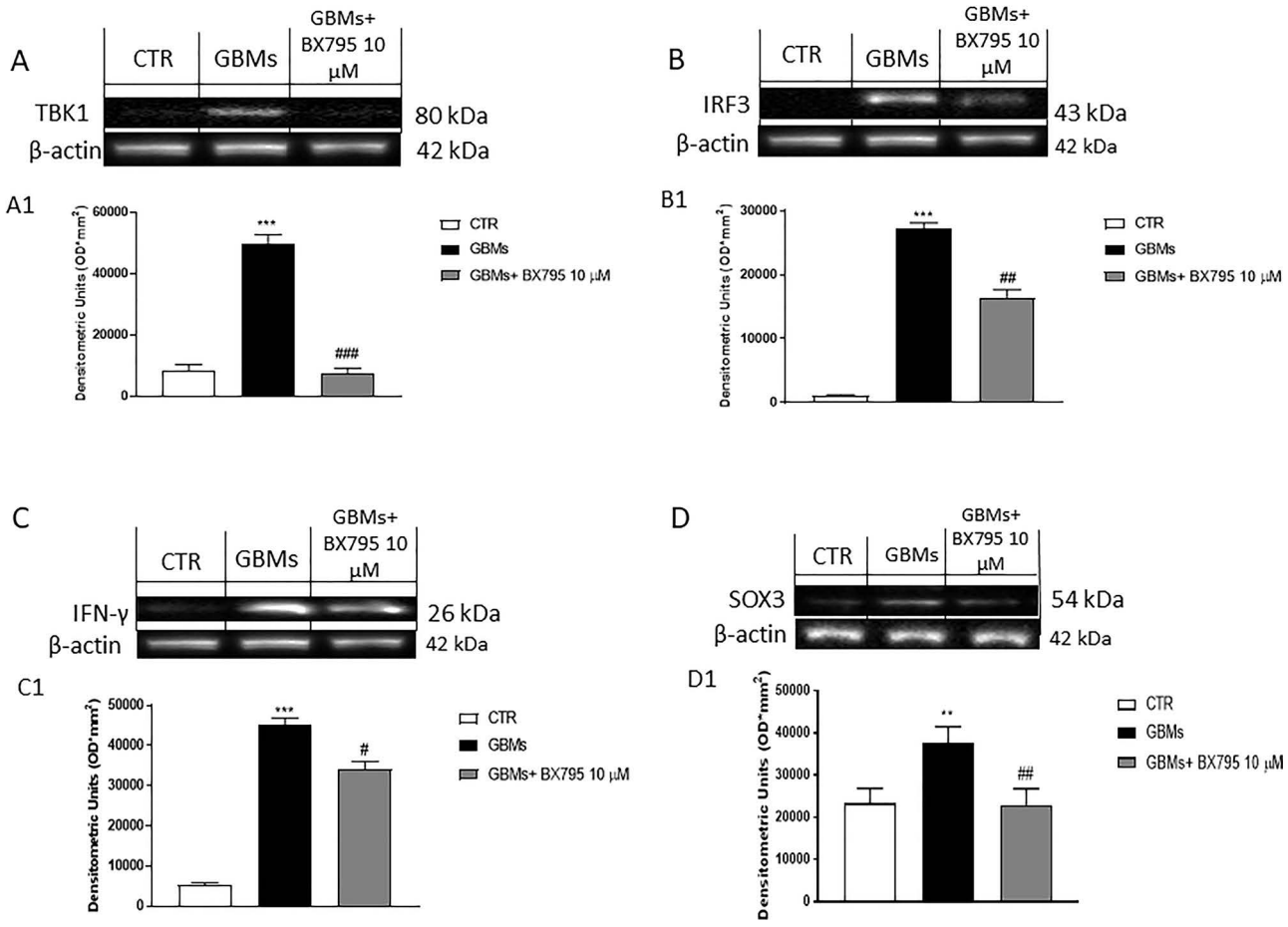

Figure 10. Effect of BX795 on TBK1, IRF3, IFN- , and SOX3 expression in primary GBM cell culture. The blot revealed an increase in TBK1 expression in primary GBM cell compared to the control group (A), confirming the TBK1 involvement in GBM pathophysiology. Meanwhile, 10 μM BX795 treatment significantly reduced its expression (A). In addition, the blot revealed an increase in IRF3, IFN- , and SOX3 expression in primary GBM cell compared to the control group. Meanwhile, 10 μM BX795 treatment significantly reduced their expression (B–D). Data are representative of at least three independent experiments: (A) ***$p < 0.001$ versus CTR, ###$p < 0.001$ versus GBMs. (B) ***$p < 0.001$ versus CTR, ##$p < 0.01$ versus GBMs. (C) ***$p < 0.001$ versus CTR; #$p < 0.05$ versus GBMs. (D) **$p < 0.01$ versus CTR; ##$p < 0.01$ versus GBMs.

are needed[33]. Previous studies have demonstrated that GBMs are highly resistant to a single inhibitor[1,34], suggesting that combination approaches, involving standard chemotherapy and pathway inhibitors, might be a possible future direction for treating GBM[35]. Molecular analysis of GBM revealed enrichment of NF- B target genes, showing that NF- B inhibition attenuated tumor proliferation and prolonged cell survival[36]. IKK , a key component of NF- B signaling, has been identified as a breast cancer oncogene; binding of IKK to the TBK1 leads to the activation of NF- B and IRF signaling pathway[7,37]. On this basis, research had identified TBK1 as an important player in the development of cancer, promoting autophagy and inflammatory processes[7,38]. Different in vitro studies demonstrated the possible use of BX795, a specific TBK1 inhibitor, for the treatment of different cancer types as primary pancreatic ductal adenocarcinoma and melanoma[10,11]. The compound BX795 was originally developed as a small-molecule inhibitor of PDK1; however, research conducted by Bain et al. demonstrated that BX795 was able to suppress mostly TBK1 and IKK [39]. In the present study, we investigated the role of BX795 on inflammation, apoptosis, and autophagy pathways in GBM. Firstly, we evaluated the cytotoxicity of BX795 at different concentrations in an in vitro model of GBM. Our results demonstrated clearly that BX795 at 1 and 10 μM significantly reduced cell viability in GBM cell lines in a concentration-dependent manner, highlighting the antiproliferative effect of BX795 treatment.

Moreover, it has been shown that TBK1 is a promoter of cancer cell survival suppressing the apoptotic pathway. GBM is characterized by altered regulation

of the apoptosis pathway, which contributes to cancer growth[1]. Apoptosis is an essential mechanism by which the homeostatic balance between cell proliferation and cell death is maintained[40]; it plays a crucial role in the development of tumors, including GBM[40]. Therefore, it has been proposed that therapeutic resistance of GBM is due to an upregulation of antiapoptotic proteins and a downregulation of proapoptotic proteins, leading to genetic instability and the activation of oncogenes that favor cell survival[41]. By evaluating apoptotic mediators such as Bax, p53, and Bcl-2, our results demonstrated that BX795 at the concentrations of 1 and 10 μM significantly reduced Bcl-2 and induced Bax and p53 expressions, promoting apoptotic process in GBM cells. Furthermore, to confirm these results, we also evaluated the involvement of specific cysteine proteases that have a key role in apoptosis such as caspase 3 and caspase 9. BX795 treatment at the concentrations of 1 and 10 μM induced caspase 3 and caspase 9 expression, confirming further apoptosis induction following BX795 treatment. GBM tumors are highly vascularized, and glioma growth depends on the formation of new blood vessels through activating oncogenes and/or downregulating tumor suppressor genes; in this field, TBK1 has been proposed as a putative mediator in tumor angiogenesis and tumor-associated microvascular inflammation[27,37]; therefore, in the present study, we investigated the role of BX795 on the angiogenesis pathway evaluating proangiogenic factors such as VEGF and IRF3. Our data clearly showed that 1 and 10 μM BX795 reduced VEGF and IRF3 expression, contrasting the development of new blood vessels and the growth of GBM.

The molecular pathogenesis of GBM is thought to involve multiple genetic alterations that result in aberrant activity of pathways involved in proliferation and inflammation[42]. Recent studies suggest an important role for NF- B signaling in GBM[43]. Increased expression of TBK1, which was observed in solid tumors, could be explained, in part, by inflammatory processes within the tumor and/or by infiltrating lymphocytes[44]. TBK1 and IKK have been studied extensively in relation to their functions in promoting the type I interferon response[7]. IKK is highly expressed in a variety of malignant tumors, and it plays an important role in tumorigenesis[45]. The binding between TBK1 and IKK promotes interferon regulatory factor (IRF3 and IRF7) phosphorylation and NF- B nuclear translocation, causing a substantial inflammatory response[7]. Therefore, in this context, we investigated the effect of BX795 on inflammatory pathway analyzing the expression of important regulatory factors of NF- B pathway, as IKK and NIK. High NIK activity is associated with different human malignancies[46]. Recent findings show that NIK promotes glioma cell invasion and tumor-associated angiogenesis[46,47]. Our results clearly demonstrated that 1 and 10 μM BX795 reduced NIK and IKK expressions in GBM cells, denoting an inhibition of the inflammatory process. To confirm the anti-inflammatory effects of BX795, we also evaluated some proinflammatory cytokine expressions such as TNF- and IFN- , demonstrating that 10 μM BX795 significantly reduced their expressions in GBM cells.

Furthermore, the current opinions regarding the role of autophagy in tumorigenesis are conflicting. Autophagy represents a highly conserved cellular homeostatic process that can have either a tumor suppressor or promoter effect depending on the tumor type and stage therapy[23]. Autophagy plays a key role in the pathogenesis of GBM[24]; cancer cells use autophagy as a cell survival mechanism, in which TBK1 appears to play a key role[24]. Specifically, TBK1 promotes Akt and p62/SQSTM1 activation, a signaling autophagy regulator factor[48], and it induces the autophagy-related (ATG) family of gene transcription such as Atg 5/12 and Atg 7. Our data demonstrated that 10 μM BX795 influenced autophagy pathway, showing a significant reduction in p62/SQSTM1, AKT, Atg 5/12, and Atg 7 activities following BX795 treatment.

Despite these promising results obtained by an in vitro model of GBM, we conducted an ex vivo model on primary GBM cell obtained from patients to confirm the effects of BX795. In accordance with the in vitro results, our data demonstrated that BX795 exerted cytotoxic effect on primary cancer cells, confirming the antiproliferative effect. Moreover, our results confirmed the direct involvement of TBK1 in GBM pathophysiology, showing also a significantly decrease in TBK1 expression after 10 μM BX795 treatment on primary GBM cell. In addition, we investigated IRF3 and IFN- expression, two key proteins phosphorylated by TBK1[29,49], demonstrating a significantly reduction in their expression following BX795 treatment. Many studies suggested also the involvement of SOX3 in tumorigenesis[31,50]; SOX3 acts as an oncogene by promoting cell proliferation, migration, and invasion[50]. High levels of SOX3 expression were detected in a subset of primary glioblastoma samples compared to nontumoral brain tissues[51]. In GBM, SOX3 is able to promote cancer cell viability and metastasis diffusion[51]. Surprisingly, our results showed a significant reduction in SOX3 expression following BX795 treatment.

In summary, the results of the present study demonstrate the involvement of the TBK1/IKK pathway in GBM pathophysiology. Furthermore, the obtained data offer new insight into the role of the NF- B and IRF signaling pathways in GBM, showing that the use of the specific TBK1/IKK inhibitor could represent a potential therapeutic treatment to counteract GBM growth, in which mortality is extremely high due to resistance to currently used therapies and the possible association of this inhibitor with the available chemotherapy to enhance its effects[52].

ACKNOWLEDGMENTS: Author contributions: S.A.S. prepared the manuscript; M.L. and G.C. performed the experiments; I.P. F.E., C.C., D.G., and S.C. analyzed the results; and E.E. and M.C. designed the study and critically revised the manuscript. All authors read and approved the final submitted version of the manuscript. This research received no external funding. The authors declare no conflicts of interest.

REFERENCES

1. Mao H, Lebrun DG, Yang J, Zhu VF, Li M. Deregulated signaling pathways in glioblastoma multiforme: Molecular mechanisms and therapeutic targets. Cancer Invest. 2012;30(1):48–56.
2. Omuro A, DeAngelis LM. Glioblastoma and other malignant gliomas: A clinical review. JAMA. 2013;310(17):1842–50.
3. Ohgaki H, Kleihues P. Epidemiology and etiology of gliomas. Acta Neuropathol. 2005;109(1):93–108.
4. Ohgaki H, Kleihues P. Population-based studies on incidence, survival rates, and genetic alterations in astrocytic and oligodendroglial gliomas. J Neuropathol Exp Neurol. 2005;64(6):479–89.
5. Stupp R, Mason WP, van den Bent MJ, Weller M, Fisher B, Taphoorn MJ, Belanger K, Brandes AA, Marosi C, Bogdahn U, Curschmann J, Janzer RC, Ludwin SK, Gorlia T, Allgeier A, Lacombe D, Cairncross JG, Eisenhauer E, Mirimanoff RO. Radiotherapy plus concomitant and adjuvant temozolomide for glioblastoma. N Engl J Med. 2005;352(10):987–96.
6. Duffau H. [Glioblastoma in 2017]. Rev Infirm. 2017;66(228):16–18.
7. Durand JK, Zhang Q, Baldwin AS. Roles for the IKK-related kinases TBK1 and IKKepsilon in cancer. Cells 2018;7(9).
8. Bishop RT, Marino S, de Ridder D, Allen RJ, Lefley DV, Sims AH, Wang N, Ottewell PD, Idris AI. Pharmacological inhibition of the IKKepsilon/TBK-1 axis potentiates the anti-tumour and anti-metastatic effects of docetaxel in mouse models of breast cancer. Cancer Lett. 2019;450:76–87.
9. Yu T, Yi YS, Yang Y, Oh J, Jeong D, Cho JY. The pivotal role of TBK1 in inflammatory responses mediated by macrophages. Mediators Inflamm. 2012;2012:979105.
10. Choi EA, Choi YS, Lee EJ, Singh SR, Kim SC, Chang S. A pharmacogenomic analysis using L1000CDS(2) identifies BX-795 as a potential anticancer drug for primary pancreatic ductal adenocarcinoma cells. Cancer Lett. 2019;465:82–93.
11. Vu HL, Aplin AE. Targeting TBK1 inhibits migration and resistance to MEK inhibitors in mutant NRAS melanoma. Mol Cancer Res. 2014;12(10):1509–19.
12. Akira S. Pathogen recognition by innate immunity and its signaling. Proc Jpn Acad Ser B Phys Biol Sci. 2009;85(4):143–56.
13. Ponten J, Macintyre EH. Long term culture of normal and neoplastic human glia. Acta Pathol Microbiol Scand. 1968;74(4):465–86.
14. Li H, Lei B, Xiang W, Wang H, Feng W, Liu Y, Qi S. Differences in protein expression between the U251 and U87 cell lines. Turk Neurosurg. 2017;27(6):894–903.
15. Ahmadipour Y, Gembruch O, Pierscianek D, Sure U, Jabbarli R. Does the expression of glial fibrillary acid protein (GFAP) stain in glioblastoma tissue have a prognostic impact on survival? Neurochirurgie 2020;66(3):150–4.
16. Restrepo A, Smith CA, Agnihotri S, Shekarforoush M, Kongkham PN, Seol HJ, Northcott P, Rutka JT. Epigenetic regulation of glial fibrillary acidic protein by DNA methylation in human malignant gliomas. Neuro Oncol. 2011;13(1):42–50.
17. Esposito E, Iacono A, Muia C, Crisafulli C, Mattace Raso G, Bramanti P, Meli R, Cuzzocrea S. Signal transduction pathways involved in protective effects of melatonin in C6 glioma cells. J Pineal Res. 2008;44(1):78–87.
18. Campolo M, Casili G, Lanza M, Filippone A, Paterniti I, Cuzzocrea S, Esposito E. Multiple mechanisms of dimethyl fumarate in amyloid beta-induced neurotoxicity in human neuronal cells. J Cell Mol Med. 2018;22(2):1081–94.
19. Irrera N, D'Ascola A, Pallio G, Bitto A, Mannino F, Arcoraci V, Rottura M, Ieni A, Minutoli L, Metro D, Mannino F, Vaccaro M, Altavilla D, Squadrito F. beta-Caryophyllene inhibits cell proliferation through a direct modulation of CB2 receptors in glioblastoma cells. Cancers (Basel) 2020;12(4):1038.
20. Talero E, Di Paola R, Mazzon E, Esposito E, Motilva V, Cuzzocrea S. Anti-inflammatory effects of adrenomedullin on acute lung injury induced by carrageenan in mice. Mediators Inflamm. 2012;2012:717851.
21. Siracusa R, Paterniti I, Impellizzeri D, Cordaro M, Crupi R, Navarra M, Cuzzocrea S, Esposito E. The association of palmitoylethanolamide with luteolin decreases neuroinflammation and stimulates autophagy in Parkinson's disease model. CNS Neurol Disord Drug Targets 2015;14(10):1350–65.
22. Esposito E, Bruscoli S, Mazzon E, Paterniti I, Coppo M, Velardi E, Cuzzocrea S, Riccardi C. Glucocorticoid-induced leucine zipper (GILZ) over-expression in T lymphocytes inhibits inflammation and tissue damage in spinal cord injury. Neurotherapeutics 2012;9(1):210–25.
23. Zhou N, Wei ZX, Qi ZX. Inhibition of autophagy triggers melatonin-induced apoptosis in glioblastoma cells. BMC Neurosci. 2019;20(1):63.
24. Kaza N, Kohli L, Roth KA. Autophagy in brain tumors: A new target for therapeutic intervention. Brain Pathol. 2012;22(1):89–98.
25. Moscat J, Karin M, Diaz-Meco MT. p62 in cancer: Signaling adaptor beyond autophagy. Cell 2016;167(3):606–9.
26. Soubannier V, Stifani S. NF-kappaB signalling in glioblastoma. Biomedicines 2017;5(2):29.
27. Ahir BK, Engelhard HH, Lakka SS. Tumor development and angiogenesis in adult brain tumor: Glioblastoma. Mol Neurobiol. 2020;57(5):2461–78.
28. Tarassishin L, Lee SC. Interferon regulatory factor 3 alters glioma inflammatory and invasive properties. J Neurooncol. 2013;113(2):185–94.
29. Bakshi S, Taylor J, Strickson S, McCartney T, Cohen P. Identification of TBK1 complexes required for the phosphorylation of IRF3 and the production of interferon beta. Biochem J. 2017;474(7):1163–74.
30. Uwanogho D, Rex M, Cartwright EJ, Pearl G, Healy C, Scotting PJ, Sharpe PT. Embryonic expression of the chicken Sox2, Sox3 and Sox11 genes suggests an interactive role in neuronal development. Mech Dev. 1995;49(1–2):23–36.
31. Xia Y, Papalopulu N, Vogt PK, Li J. The oncogenic potential of the high mobility group box protein Sox3. Cancer Res. 2000;60(22):6303–6.
32. Forte IM, Indovina P, Iannuzzi CA, Cirillo D, Di Marzo D, Barone D, Capone F, Pentimalli F, Giordano A. Targeted therapy based on p53 reactivation reduces both glioblastoma cell growth and resistance to temozolomide. Int J Oncol. 2019;54(6):2189–99.

33. Cruickshanks N, Zhang Y, Yuan F, Pahuski M, Gibert M, Abounader R. Role and therapeutic targeting of the HGF/MET pathway in glioblastoma. Cancers (Basel) 2017;9(7):87.
34. Friedman HS, Kerby T, Calvert H. Temozolomide and treatment of malignant glioma. Clin Cancer Res. 2000;6(7):2585–97.
35. Sasmita AO, Wong YP, Ling APK. Biomarkers and therapeutic advances in glioblastoma multiforme. Asia Pac J Clin Oncol. 2018;14(1):40–51.
36. Friedmann-Morvinski D, Narasimamurthy R, Xia Y, Myskiw C, Soda Y, Verma IM. Targeting NF-kappaB in glioblastoma: A therapeutic approach. Sci Adv. 2016;2(1):e1501292.
37. Czabanka M, Korherr C, Brinkmann U, Vajkoczy P. Influence of TBK-1 on tumor angiogenesis and microvascular inflammation. Front Biosci. 2008;13:7243–9.
38. Ma X, Helgason E, Phung QT, Quan CL, Iyer RS, Lee MW, Bowman KK, Starovasnik MA, Dueber EC. Molecular basis of tank-binding kinase 1 activation by transautophosphorylation. Proc Natl Acad Sci USA 2012;109(24):9378–83.
39. Bain J, Plater L, Elliott M, Shpiro N, Hastie CJ, McLauchlan H, Klevernic I, Arthur JS, Alessi DR, Cohen P. The selectivity of protein kinase inhibitors: A further update. Biochem J. 2007;408(3):297–315.
40. Goldar S, Khaniani MS, Derakhshan SM, Baradaran B. Molecular mechanisms of apoptosis and roles in cancer development and treatment. Asian Pac J Cancer Prev. 2015;16(6):2129–44.
41. Krakstad C, Chekenya M. Survival signalling and apoptosis resistance in glioblastomas: Opportunities for targeted therapeutics. Mol Cancer 2010;9:135.
42. Cancer Genome Atlas Research Network. Comprehensive genomic characterization defines human glioblastoma genes and core pathways. Nature 2008;455(7216):1061–8.
43. Karin M, Cao Y, Greten FR, Li ZW. NF-kappaB in cancer: From innocent bystander to major culprit. Nat Rev Cancer 2002;2(4):301–10.
44. Cai X, Chiu YH, Chen ZJ. The cGAS–cGAMP–STING pathway of cytosolic DNA sensing and signaling. Mol Cell 2014;54(2):289–96.
45. Yin M, Wang X, Lu J. Advances in IKBKE as a potential target for cancer therapy. Cancer Med. 2020;9(1):247–58.
46. Cherry EM, Lee DW, Jung JU, Sitcheran R. Tumor necrosis factor-like weak inducer of apoptosis (TWEAK) promotes glioma cell invasion through induction of NF-kappaB-inducing kinase (NIK) and noncanonical NF-kappaB signaling. Mol Cancer 2015;14:9.
47. Duran CL, Lee DW, Jung JU, Ravi S, Pogue CB, Toussaint LG, Bayless KJ, Sitcheran R. NIK regulates MT1-MMP activity and promotes glioma cell invasion independently of the canonical NF-kappaB pathway. Oncogenesis 2016;5(6):e231.
48. Herhaus L, Bhaskara RM, Lystad AH, Gestal-Mato U, Covarrubias-Pinto A, Bonn F, Simonsen A, Hummer G, Dikic I. TBK1-mediated phosphorylation of LC3C and GABARAP-L2 controls autophagosome shedding by ATG4 protease. EMBO Rep. 2020;21(1):e48317.
49. Guinn ZP, Petro TM. Interferon regulatory factor 3 plays a role in macrophage responses to interferon-gamma. Immunobiology 2019;224(4):565–74.
50. Dong C, Wilhelm D, Koopman P. Sox genes and cancer. Cytogenet Genome Res. 2004;105(2–4):442–7.
51. Marjanovic Vicentic J, Drakulic D, Garcia I, Vukovic V, Aldaz P, Puskas N, Nikolic I, Tasic G, Raicevic S, Garros-Regulez L, Aldaz P, Sampron N, Atkinson MJ, Anastasov N, Matheu A, Stevanovic M. SOX3 can promote the malignant behavior of glioblastoma cells. Cell Oncol. (Dordr) 2019;42(1):41–54.
52. Choi JI, Park SH, Lee HJ, Lee DW, Lee HN. Inhibition of phospho-S6 kinase, a protein involved in the compensatory adaptive response, increases the efficacy of paclitaxel in reducing the viability of matrix-attached ovarian cancer cells. PLoS One 2016;11(5):e0155052.